

Spatiotemporal Dependable Task Execution Services in MEC-enabled Wireless Systems

Mustafa Emara, *Student Member, IEEE*, Hesham ElSawy, *Senior Member, IEEE*, Miltiades C. Filippou, *Senior Member, IEEE*, Gerhard Bauch, *Fellow, IEEE*

Abstract—Multi-access Edge Computing (MEC) enables computation and energy-constrained devices to offload and execute their tasks on powerful servers. Due to the scarce nature of the spectral and computation resources, it is important to jointly consider i) contention-based communications for task offloading and ii) parallel computing and occupation of failure-prone MEC processing resources (virtual machines). The feasibility of task offloading and successful task execution with virtually no failures during the operation time needs to be investigated collectively from a combined point of view. To this end, this letter proposes a novel spatiotemporal framework that utilizes stochastic geometry and continuous time Markov chains to jointly characterize the communication and computation performance of dependable MEC-enabled wireless systems. Based on the designed framework, we evaluate the influence of various system parameters on different dependability metrics such as (i) computation resources availability, (ii) task execution retainability, and (iii) task execution capacity. Our findings showcase that there exists an optimal number of virtual machines for parallel computing at the MEC server to maximize the task execution capacity.

Index Terms—Multi-access edge computing, virtual machines, queueing theory, stochastic geometry, dependability.

I. INTRODUCTION

The deployment of Multi-access Edge Computing (MEC) in 5G and beyond systems allows applications to be instantiated at the edge of the network. As a direct benefit, efficient task execution is feasible due to the MEC servers high computation power [1]. A major challenge for network operators is to provide dependable and ubiquitous computing services that meet the computing demands of devices running various heterogeneous applications (e.g., artificial intelligence, Blockchain, automotive and E-health). Efficient spectrum access for task offloading along with parallel task computation at the MEC server are required to jointly meet such heterogeneous application requirements [2]. To ensure efficient operation, the task offloading feasibility, computation resources availability, and task execution retainability ought to be jointly quantified and optimized [3].

In MEC-enabled networks, task execution at the MEC server is strongly tied to the resources availability and the resilience to failures [4]. In this context, various cloud-based

provisioning and resilience schemes are discussed in [5]. Causes of service disruption due to physical machines (PMs) and virtual machines (VMs) failures along with their analysis are provided in [6]. With regard to wireless-based task offloading, [7] examines the network scalability and identifies communication and computation performance frontiers. Heterogeneous networks analysis is presented in [8], where the network-wide outage probability is derived for task offloading assuming different computation architectural variants. Authors in [9] proposed a transmission and energy efficient offloading algorithm based on a Markov decision process that accounts for the spatial and temporal network parameters.

However, the aforementioned works either exclusively consider a dependability view of the network [4]–[6], or a spatiotemporal one [7]–[9]. As a result, the problem of feasible and dependable task execution, accounting for the joint limitation of network-wide mutual interference and parallel task computing by failure-prone VMs is still not addressed. Motivated by the above, we propose a spatiotemporal feasibility-assessment framework that entails network-wide mutual interference and temporal-based task arrivals/ processing in uplink MEC-enabled networks. Furthermore, we adopt an individual (i.e., per-task and per-device) task execution criterion that aims to exploit the computation resources at the MEC server if the radio conditions permit. Our analysis is then followed by the assessment of new service dependability-relevant key performance indicators (KPIs) that shed light on the system availability and task execution capability.

II. SYSTEM MODEL

1) **Network model:** We consider a cellular uplink network, where the base stations (BSs) and devices are spatially deployed in \mathbb{R}^2 according to two independent homogeneous Poisson point processes (PPPs), denoted by Ψ and Φ with intensities λ_b and λ_d , respectively. An unbounded path-loss propagation model is adopted such that the signal power attenuates at rate of $r^{-\eta}$, where r is the distance and η is the path-loss exponent. Wireless links are assumed to undergo Rayleigh fading, where the power gains of the signal of interest h and the interference signal g , are exponentially distributed with unit power gain. Full path-loss channel inversion power control is adopted, which implies that all devices adjust their transmit powers such that the received uplink power levels at the BS are equal to a predetermined threshold ρ .

2) **Offloading model:** We consider a continuous time system where task arrivals at each device are modeled via an independent Poisson process with rate λ_a tasks/ unit time.

M. Emara and Miltiades C. Filippou are with the Germany standards R&D team, Next Generation and Standards, Intel Deutschland GmbH, 85579 Neubiberg, Germany (e-mail: mustafa.emara, miltiadis.filippou@intel.com)

H. ElSawy is with the Electrical Engineering Department, King Fahd University of Petroleum and Minerals, 31261 Dhahran, Saudi Arabia (email: hesham.elsawy@kfupm.edu.sa).

G. Bauch and M. Emara are with the Institute of Communications, Hamburg University of Technology, Hamburg, 21073 Germany (email: bauch@tuhh.de).

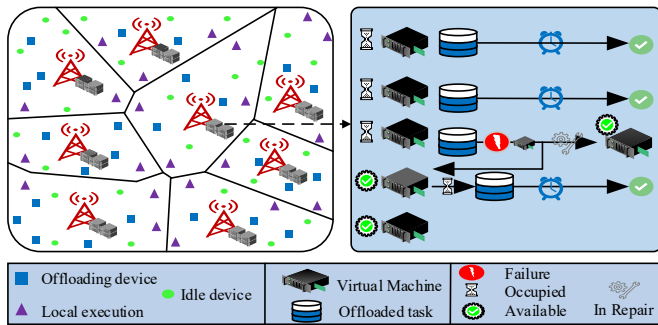


Fig. 1: The considered system model with 5 VMs deployed.

Proactively, devices attempt to offload generated tasks by sending instructions to a MEC server collocated with the connected BS. In our system, grant-free access is assumed, where each device attempts to transmit its task instruction (i.e., not the whole task) using one of the available C uplink channels randomly and uniformly without a scheduling grant from the BS [10]. Furthermore, let $\kappa = \frac{\lambda_d}{\lambda_b C}$ denote the average number of devices per BS per channel and T_s the transmission time of a given task's instruction. A task instruction is successfully decoded at the BS if its received signal to interference plus noise ratio (SINR) is larger than a predefined threshold, θ . The offloading success probability (OSP) of a generic device, which is denoted by \mathcal{O} , quantifies the probability of successful task offloading as $\mathcal{O} = \mathbb{P}\{\text{SINR} > \theta\}$.¹ In the case of decoding failure (i.e., NACK is received), the device opts to compute its task locally. Accordingly, we adopt a *coverage-based* offloading feasibility criterion, in which the OSP \mathcal{O} governs the offloading feasibility, thus, the offloading decision problem and its underlying parameters are not considered and left for future work. Retransmissions at the devices are not considered in the proposed model to lower the aggregate network-wide interference.

3) **Computing model:** The MEC server residing at each BS is equipped with a single PM that encompasses M_{MEC} VMs for parallel task computing. To account for resource sharing among the VMs (e.g., buses for I/O, CPU, memory), input/output (I/O) interference is observed within the PM at the MEC server. Thus, the parallel-operating VMs interfere with each other, leading to a degraded computation power [11]. For the case of a single VM deployment, the task's execution rate is modeled via a Poisson process with a rate of μ_o tasks/ unit time. However, to account for the I/O interference among the M_{MEC} VMs, the task's execution rate of a given VM depends on the total number of VMs as follows

$$\mu_{\text{MEC}} = \frac{\mu_o}{(1+d)^{M_{\text{MEC}}-1}}, \quad (1)$$

where d is the computation degradation factor due to I/O interference among the M_{MEC} VMs [7], [11]. For local computation of tasks, devices are assumed to be equipped with a local PM that accommodates a single VM (i.e., $M_{\text{loc}} = 1$, thus, no parallel processing), where the local execution rate is modeled via a Poisson process with rate μ_{loc} . Moreover,

¹ACK and NACK transmission latencies are ignored as they incur negligible amount compared to T_s and the task's execution time.

a task to be computed is blocked if no VM is idle (locally or at the MEC server in case of offloading). To investigate the relative ratio between the MEC and the local computation capabilities, we define $\mu_r = \mu_{\text{MEC}}/\mu_{\text{loc}}$ which denotes the relative computation rate such that $\mu_r \gg 1$.

4) **Failure & repair model:** Due to possible hardware and software faults, the proposed model accounts for events of VM failures and their repairment times [6], [12]. The failure (repair) rate of a given VM is modeled via a Poisson process with rate δ (γ) failure (repairment) events/ unit time.² VMs are prone to failure regardless of being idle or occupied. A failed idle VM is labeled as out of operation and cannot admit future tasks. Upon the failure of an occupied VM, the PM will handover the running task to an idle VM, if one exists. If not, the running task is discarded and the concerned device is notified via downlink signaling. The considered system model is visualized in Fig. 1, where one can observe a plethora of devices belonging to three categories, namely, idle, offloading and local execution devices. Focusing on a selected cell that serves a number of offloading devices, a VM fails while being in service. In this case, the task being served by this VM is transferred to an idle VM to resume its execution. Meanwhile, based on the repair rate, the failed VM goes back into operation to serve newly incoming tasks.

III. SPATIAL SYSTEM ANALYSIS

In our work, we focus on critical applications that are sensitive to availability and reliability of the computation resources (e.g., smart agriculture, smart homes [2]), whereas latency-critical applications are left for future work. Upon task generation, the task instructions are sent to the MEC host co-located with the connected BS by uplink transmissions. Those instructions are correctly decoded, and hence the task is successfully offloaded, if the received SINR is greater than θ . Otherwise, the device executes the task locally. To characterize the offloading feasibility within the network, the OSP of a randomly selected device considering the network-wide mutual interference is

$$\mathcal{O} = \mathbb{P} \left\{ \frac{\rho h_o}{\sum_{y_n \in \Phi \setminus y_o} a_n P_n g_n \|y_n - z_o\|^{-\eta} + \sigma^2} > \theta \right\}, \quad (2)$$

$$\stackrel{(a)}{=} \exp \left\{ -\frac{\sigma^2 \theta}{\rho} \right\} \mathcal{L}_{I_{\text{out}}} \left(\frac{\theta}{\rho} \right) \mathcal{L}_{I_{\text{in}}} \left(\frac{\theta}{\rho} \right). \quad (3)$$

where h_o is the channel gain between the intended device located at y_o and its serving BS located at z_o , $\|\cdot\|$ is the Euclidean norm, y_n is the n -th device location in the network excluding the intended device, P_n is its transmit power, g_n is the channel power gain between this interfering device and the intended BS, σ^2 is the noise power and a_n equals one if the n -th device is transmitting on the same channel as the intended device, and zero otherwise. In addition, (a) results from the exponential distribution of h_o combined with the path loss inversion power control, where $\mathcal{L}_{I_{\text{out}}}(\cdot)$ and $\mathcal{L}_{I_{\text{in}}}(\cdot)$ represent the Laplace transform (LT) of the aggregate intra-cell and inter-cell interference, respectively. To provide an

²The Poisson model is adopted in our work for task-related parameters to provide a good compromise between practical consideration of real-time events and mathematical tractability [7], [8].

uplink tractable analysis, we assume that the spatial correlations between adjacent Voronoi cell areas are ignored, thus, the transmission powers of the devices are independent and identically distributed [13]. The aforementioned approximations are validated in Section V against independent Monte Carlo simulations. In order to quantify the total arrival rate of offloaded tasks at the MEC server, the OSP of each device is first calculated in the following theorem.

Theorem 1. *The OSP for a generic device is given by*

$$\mathcal{O} \approx \frac{\exp\left\{-\frac{\sigma^2\theta}{\rho} - \frac{2\theta P_a \kappa}{(\eta-2)} {}_2F_1(1, 1-2/\eta, 2-2/\eta, -\theta)\right\}}{\left(1 + \frac{\theta P_a \kappa}{(1+\theta)c}\right)^c}$$

$$\stackrel{(\eta \equiv 4)}{=} \frac{\exp\left\{-\frac{\sigma^2\theta}{\rho} - P_a \kappa \sqrt{\theta} \arctan(\sqrt{\theta})\right\}}{\left(1 + \frac{\theta P_a \kappa}{(1+\theta)c}\right)^c}, \quad (4)$$

where $P_a = 1 - e^{-(2T_s \lambda_a)}$ is the device's active probability within $[-T_s, T_s]$, $\kappa = \frac{\lambda_d}{\lambda_b c}$, ${}_2F_1(\cdot)$ is the Gaussian hypergeometric function and $c = 3.575$. The approximation is due to the employed approximate probability distribution function (PDF) of the PPP Voronoi cell area in \mathbb{R}^2 .

Proof. Since full channel inversion power control with threshold ρ is employed, the received power from the devices at a given BS equals ρ and the interference power from the neighboring devices is strictly lower than ρ . Thus, the LT of the aggregate inter-cell interference at the serving BS is

$$\mathcal{L}_{I_{\text{out}}}(s) \approx \exp\left(-2\pi P_a \lambda_d s^{\frac{2}{\eta}} \mathbb{E}\left\{[P_{\frac{2}{\eta}}]^{\frac{2}{\eta}}\right\} \int_{(s\rho)^{-\frac{1}{\eta}}}^{\infty} \frac{y}{y^n + 1} dy\right), \quad (5)$$

where $P_a \lambda_d$ represent the portion of active devices within the network and the approximation is due to the assumed independent transmission powers of the devices. The LT of the inter-cell interference can be evaluated as [13, Lemma 1]

$$\mathcal{L}_{I_{\text{in}}}(s) \approx \mathbb{P}\{\mathcal{N}_d = 0\} + \sum_{n=1}^{\infty} \frac{\mathbb{P}\{\mathcal{N}_d = n\}}{(1+s\rho)^n} \quad (6)$$

where $\mathbb{E}\{\cdot\}$ is the expectation operation, \mathcal{N}_d is a random variable representing the number of neighboring devices with the probability mass function $\mathbb{P}\{\mathcal{N}_d = n\} \approx \frac{\lambda_d^n (\lambda_b c)^c \Gamma(n+c)}{(\lambda_d + \lambda_b c)^{n+c} \Gamma(n+1) \Gamma(c)}$, where $\Gamma(\cdot)$ is the gamma function and $c = 3.575$ is a constant defined to approximate the Voronoi cell. The theorem is proved by plugging (5) and (6) into (3), followed by similar steps as done in [13, Lemma 1]. ■

Once \mathcal{O} is evaluated, we can now define and evaluate the related task execution KPIs for the case of offloaded and locally executed tasks as explained in the following section.

IV. TEMPORAL COMPUTATIONAL ANALYSIS

As explained earlier, the OSP provides an offloading feasibility assessment via controlling the aggregate load of tasks at the MEC server. That is, the total average arrival rate of tasks to be computed at the MEC server is $\lambda_{\text{MEC}} = \mathcal{O} \lambda_a \mathbb{E}\{\mathcal{N}_d\} = \frac{\mathcal{O} \lambda_a \lambda_d}{\lambda_b}$. On the other hand, the average arrival rate of tasks to be locally computed is $\lambda_{\text{loc}} = \bar{\mathcal{O}} \lambda_a$ tasks/ unit time, where $\bar{\mathcal{O}} = 1 - \mathcal{O}$. To analyze the temporal occupancy of the VMs

either locally or at the MEC server, we employ tools from queueing theory. To construct the proposed continuous time Markov chain (CTMC), we first determine the system's state space. A general state of our model is represented by the tuple $z = (x_I, x_O, x_F)$; where $x_i; i \in \{I, O, F\}$ represents the number of VMs that are idle, occupied and failed, respectively. Let $\mathcal{S}_v = \left\{z \mid \sum_j x_j = M_v; j \in \{I, O, F\}\right\}$ denote the state space, where $v \in \{\text{MEC}, \text{loc}\}$ denotes the MEC and local systems. The steady state equations can be vectorized as $\boldsymbol{\tau}_v = [\tau_1 \ \tau_2 \ \cdots \ \tau_\ell \ \cdots \ \tau_{|\mathcal{S}_v|}]$, where τ_ℓ is the probability of being in the ℓ -th state. For full temporal characterization, we need to construct the state transition matrix \mathbf{Q}_v . For each system v , \mathbf{Q}_v constitutes the transition rates associated with different states. To systematically construct \mathbf{Q}_v , while taking into account the different temporal events, Table I is utilized, which entails the transition rates and conditions among different system states. Focusing in this work on the steady state solution, the steady state probabilities are evaluated via solving $\boldsymbol{\tau}_v \mathbf{Q}_v = 0$, and $\sum_{z \in \mathcal{S}_v} \tau_v(z) = 1$. Let $\mathbf{1}$ and \mathcal{I} denote the all ones vector and the all ones matrix, with the appropriate sizes respectively, then, $\boldsymbol{\tau}_v$ equals $\boldsymbol{\tau}_v = \mathbf{1}(\mathbf{Q}_v + \mathcal{I})^{-1}$. Once the solution $\boldsymbol{\tau}_v$ is obtained, several dependability-based KPIs can be assessed. First, we consider the *computation resource availability (CRA)*. This metric quantifies the probability that an incoming device's task, either locally managed or offloaded to the MEC server, finds a vacant computational resource. First, let $\mathcal{N}_v = \{z \mid x_I = 0, z \in \mathcal{S}_v\}$ denote all states with no idle VMs. Then, the CRA, denoted as A , can be evaluated as

$$A = \mathcal{O} \left(1 - \sum_{z \in \mathcal{N}_{\text{MEC}}} \tau_{\text{MEC}}(z)\right) + \bar{\mathcal{O}} \left(1 - \sum_{z \in \mathcal{N}_{\text{loc}}} \tau_{\text{loc}}(z)\right). \quad (7)$$

Another important KPI that quantifies the degree of successful task execution, is the *task execution capacity (TEC)*. Let $\mathcal{C}_v = \{z \mid x_O > 0, z \in \mathcal{S}_v\}$ denote all states with at least a single occupied VM. The TEC considers such states to evaluate the system's capability to perform task execution successfully. Denoted by C , the TEC can be computed as

$$C = \mathcal{O} \mu_{\text{MEC}} \sum_{z \in \mathcal{C}_{\text{MEC}}} x_O \tau_{\text{MEC}}(z) + \bar{\mathcal{O}} \mu_{\text{loc}} \sum_{z \in \mathcal{C}_{\text{loc}}} x_O \tau_{\text{loc}}(z). \quad (8)$$

Finally, we consider the *task execution retainability (TER)*, which is defined as the probability that a task, once assigned to a VM, will be computed successfully without interruption [14]. Mathematically, the TER, denoted by R_v , can be evaluated as $R_v = 1 - \frac{F_v}{\Lambda_v}$, where F_v denotes the mean forced termination rate of ongoing tasks and Λ_v is the effective rate in which a new task is assigned to an idle VM. The latter can be computed similar to (7) as $\Lambda_v = \lambda_v (1 - \sum_{z \in \mathcal{N}_v} \tau_v(z))$. Moreover, let $\mathcal{F}_v = \mathcal{C}_v \cup \mathcal{N}_v$ denote all states with at least a single occupied VM and no idle VMs. Tasks that are interrupted in those states, because of VM failures, are dropped. Finally, F_v and the TER are evaluated as

$$F_v = \delta \sum_{z \in \mathcal{F}_v} (M_v - x_F) \tau_v(z), \quad (9)$$

$$R = \mathcal{O} \left(1 - \frac{F_{\text{MEC}}}{\Lambda_{\text{MEC}}}\right) + \bar{\mathcal{O}} \left(1 - \frac{F_{\text{loc}}}{\Lambda_{\text{loc}}}\right). \quad (10)$$

TABLE I: State transitions $z = (x_I, x_O, x_F)$ of the VMs.

Event	Destination state	Transition rate	Necessary condition
1- Task arrival and an idle VM is allocated	$(x_I - 1, x_O + 1, x_F)$	λ_v	$x_I > 0$
2- Successful task execution at an occupied VM	$(x_I + 1, x_O - 1, x_F)$	$x_O \mu_v$	$x_O > 0$
3- An idle VM fails	$(x_I - 1, x_O, x_F + 1)$	$x_I \delta$	$x_I > 0$
4- An occupied VM fails. Task is offloaded to another idle VM	$(x_I - 1, x_O - 1, x_F + 1)$	$x_O \delta$	$x_O > 0 \ \& \ x_I > 0$
5- An occupied VM fails and task is aborted	$(x_I, x_O - 1, x_F + 1)$	$x_O \delta$	$x_O > 0 \ \& \ x_I = 0$
6- A failed VM is repaired	$(x_I + 1, x_O, x_F - 1)$	$x_F \gamma$	$x_F > 0$

Algorithm 1 Optimal number of deployed VMs computation.

Input $(P_a, \lambda_a, \lambda_b, \lambda_d, M_{\text{MEC}}, M_{\text{loc}}, \mu_o, \mu_{\text{loc}}, d, \gamma, \delta)$
 | Set $m = 1, C(0) = -\infty$, and compute $C(m) \triangleright R(m)$
 implies computing C in (8) with $M_{\text{MEC}} = m$.
 | **while** $C(m) > C(m - 1)$ **do**
 | | Compute $C(m)$ from (8).
 | | Increment m .
 | **end while**
Output: $M_{\text{MEC}}^* = m$ and $C^* = C(M_{\text{MEC}}^*)$.
end Input

TABLE II: Simulation parameters.

Parameter	value
Average number of BSs (devices) $(\lambda_b (\lambda_d))$	1 (64) BS (device)/ 10 km ²
Number of VMs $(M_{\text{MEC}}, M_{\text{loc}})$	5, 1
Number of uplink channels (C)	16
Uplink power control threshold (ρ)	-90 dBm
Path-loss exponent (η)	4
Noise power (σ^2)	-110 dBm
Detection threshold (θ)	-10 dB
Task arrival rate per device (λ_a)	0.15 tasks/ unit time
Single VM execution rate (μ_o)	3 tasks/ unit time
Local execution rate (μ_{loc})	0.1 tasks/ unit time
VM repair rate (δ)	1 events/ unit time
VM failure rate (γ)	0.1 events/ unit time
VM I/O degradation factor (d)	0.1

V. NUMERICAL RESULTS

This section aims to numerically evaluate the proposed task execution service dependability KPIs focusing on the studied MEC-enabled network. Unless otherwise stated, the list of involved network parameters are summarized in Table II.

Fig. 2 shows the OSP as a function of the decoding threshold θ for different device active probabilities P_a . The close match between the simulation and the proposed analytical framework validates the analysis and justifies the considered approximations. For increasing values of θ , the OSP decreases due to higher requirement on the link quality. For increasing values of P_a , the rate of task generation at the devices as well as their the probability to utilize the same uplink channel increases, thus network-wide mutual interference increases, hence, leading to lower achievable OSPs.

Focusing on the introduced KPIs in Section IV, Fig. 3 showcases the system's performance for increasing values of θ with different system parameters. Generally, as θ increases, the OSP decreases, thus, owing to the coverage-based offloading criterion, more devices opt to execute their tasks locally. Depending on \mathcal{O} , which depends on θ among other parameters, the network oscillates between an *offloading-dominant* and a *local execution-dominant* regime. In Fig. 3(a), we observe that the CRA keeps increasing till a cut-off threshold (i.e., $\theta = -6, -7$ and -8 dB for $\mu_r = 20, 40, 80$,

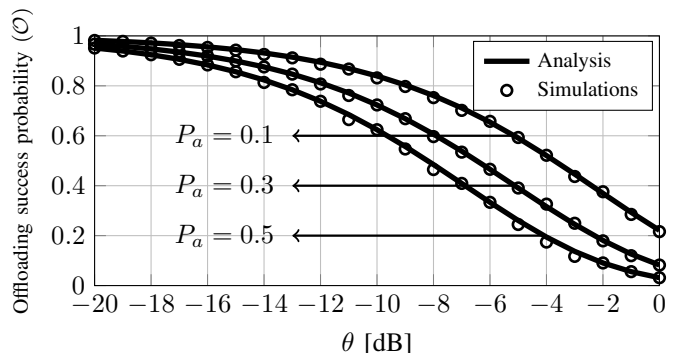


Fig. 2: OSP model verification.

respectively). Operating above these threshold values, the network transitions to the local execution-dominant regime. As μ_r decreases, the CRA performance gap between the two regimes decreases, since the computational capabilities of the MEC server and device become comparable. Fig. 3(b) presents the TER for different per-device task arrival rates. As λ_a increases, the contention on the radio and the computational resources increases, leading to degradation in the TER. Fig. 3(c) shows the TEC for different densification ratios (i.e., average number of devices per BS per channel). In the offloading-dominant regime, high values of TEC are achieved since the offloaded tasks leverage the computationally capable MEC server. However, in the local execution-dominant regime, TEC degrades till it reaches zero. We observe also the effect of κ on the slope steepness of each curve.

The computation resources scalability is depicted via Fig. 4 which shows the TEC as a function of the number of MEC server VMs M_{MEC} and for three different values of the computation degradation factor d . The optimal number of deployed VMs for each value of d , calculated via Algorithm 1, which has a complexity of $O(M_{\text{MEC}})$, is shown via red circles. It is worth mentioning that the values present in Table II result in $P_a = 0.25$ and $p = 0.83$. Thus, around 83% of the active devices will offload their generated tasks to the MEC server, thus, operating at the offloading-dominant regime. Nevertheless, due to the I/O interference between the employed VMs at the MEC server, increasing M_{MEC} beyond a given value, depending on the value of parameter d , leads to degradation in μ_{MEC} till the VM I/O interference dominates and the TEC approaches zero. Such behavior also explains why as d decreases, higher numbers of VMs are desirable. These performance results provide network operators with important insights regarding the network dimensioning.

Finally, Fig. 5 shows the TER as a function of the repair

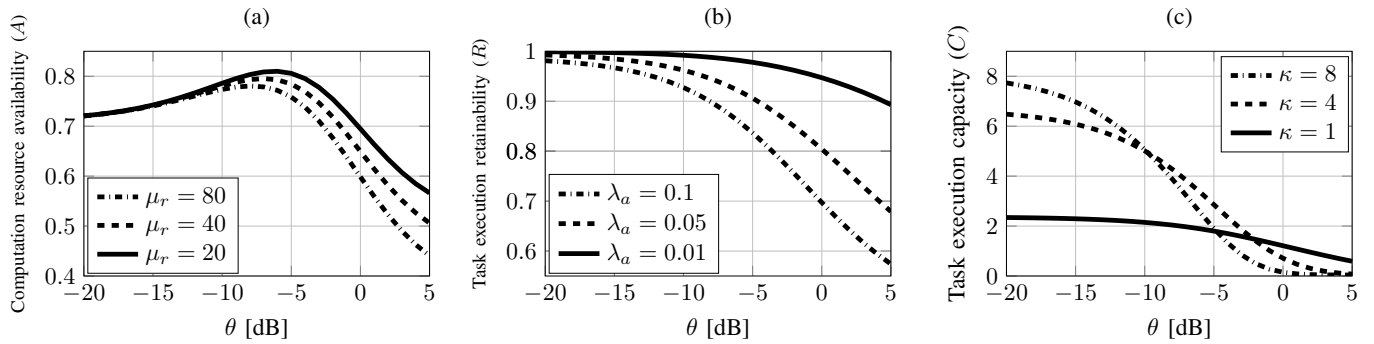


Fig. 3: Steady state (a) CRA with relative computation ratios (b) TER with task arrival rates (c) TEC with densification ratios.

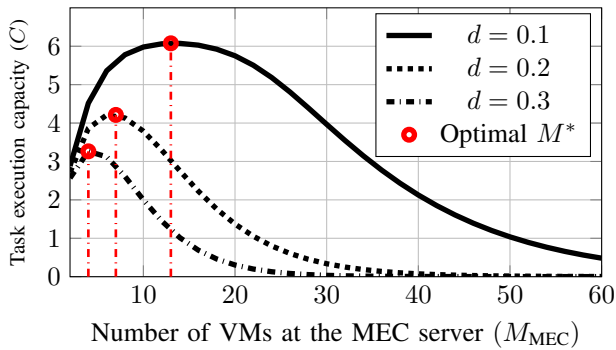


Fig. 4: TEC as a function of number of VMs (M_{MEC}).

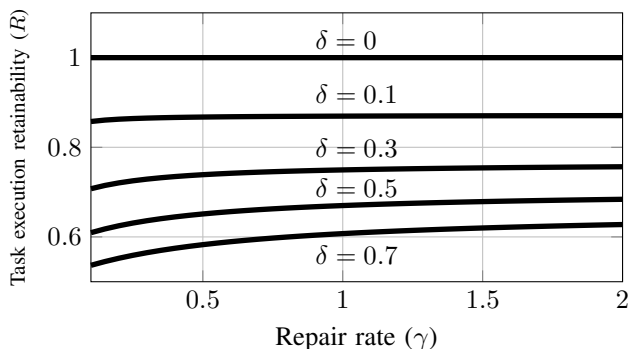


Fig. 5: TER as a function of repair rate γ .

rate γ for different values of failure rate δ . For the extreme case of $\delta = 0$, the TER equals 1, independent of γ , since no VM will ever fail. As δ increases, we observe the impact of the repair rate on the TER, especially within the range $\gamma \in [0, 1]$. For higher values of γ , the TER starts to saturate, owing to its superiority over δ , which yields it insignificant with respect to the TER.

VI. CONCLUSION

This letter presents a spatiotemporal framework to characterize the network-wide task execution from a dependability perspective considering a coverage-based offloading feasibility criterion. Modeling tools are utilized to derive mathematical expressions of the OSP and a number of novel task execution dependability-based KPIs, such as CRA, TER and TEC. To yield the framework practical, VMs failures and repairment events are considered. Numerical results showcase

regimes where the system transitions from the *offloading-dominant* to the *local execution-dominant* regime. Different system parameters such as task arrival rate, densification ratio and VM computation capabilities, are presented to obtain an understanding of the system's behavior. Finally, we show that assuming a given parameterization, there exists an optimal number of VMs, which, when deployed, maximizes the TEC.

REFERENCES

- [1] P. Mach *et al.*, "Mobile edge computing: A survey on architecture and computation offloading," *IEEE Communications Surveys Tutorials*, vol. 19, no. 3, pp. 1628–1656, third quarter 2017.
- [2] P. Porambage *et al.*, "Survey on multi-access edge computing for internet of things realization," *IEEE Communications Surveys Tutorials*, vol. 20, no. 4, pp. 2961–2991, 2018.
- [3] M. Bennis *et al.*, "Ultrareliable and low-latency wireless communication: Tail, risk, and scale," *Proceedings of the IEEE*, vol. 106, no. 10, pp. 1834–1853, 2018.
- [4] S. Bagchi *et al.*, "Dependability in edge computing," *Communications of the ACM*, vol. 63, no. 1, pp. 58–66, 2020.
- [5] C. Colman-Meixner *et al.*, "A survey on resiliency techniques in cloud computing infrastructures and applications," *IEEE Communications Surveys Tutorials*, vol. 18, no. 3, pp. 2244–2281, 2016.
- [6] R. Birke *et al.*, "Failure analysis of virtual and physical machines: Patterns, causes and characteristics," in *2014 44th Annual IEEE International Conference on Dependable Systems and Networks*, 2014.
- [7] S. Ko *et al.*, "Wireless networks for mobile edge computing: Spatial modeling and latency analysis," *IEEE Transactions on Wireless Communications*, vol. 17, no. 8, pp. 5225–5240, Aug 2018.
- [8] H. Lee *et al.*, "Task offloading in heterogeneous mobile cloud computing: Modeling, analysis, and cloudlet deployment," *IEEE Access*, vol. 6, pp. 14 908–14 925, 2018.
- [9] H. Ko *et al.*, "Spatial and temporal computation offloading decision algorithm in edge cloud-enabled heterogeneous networks," *IEEE Access*, vol. 6, pp. 18 920–18 932, 2018.
- [10] N. H. Mahmood *et al.*, "Uplink grant-free access solutions for urllc services in 5g new radio," in *2019 16th International Symposium on Wireless Communication Systems (ISWCS)*, 2019, pp. 607–612.
- [11] D. Bruneo, "A stochastic model to investigate data center performance and QoS in IaaS cloud computing systems," *IEEE Transactions on Parallel and Distributed Systems*, vol. 25, no. 3, pp. 560–569, 2014.
- [12] S. Fu, "Failure-aware construction and reconfiguration of distributed virtual machines for high availability computing," in *9th IEEE/ACM International Symposium on Cluster Computing*, 2009, pp. 372–379.
- [13] M. Gharbieh *et al.*, "Spatiotemporal stochastic modeling of IoT enabled cellular networks: Scalability and stability analysis," *IEEE Transactions on Communications*, vol. 65, no. 8, pp. 3585–3600, Aug 2017.
- [14] I. A. M. Balapuwaduge *et al.*, "Dynamic spectrum reservation for cr networks in the presence of channel failures: Channel allocation and reliability analysis," *IEEE Transactions on Wireless Communications*, vol. 17, no. 2, pp. 882–898, 2018.